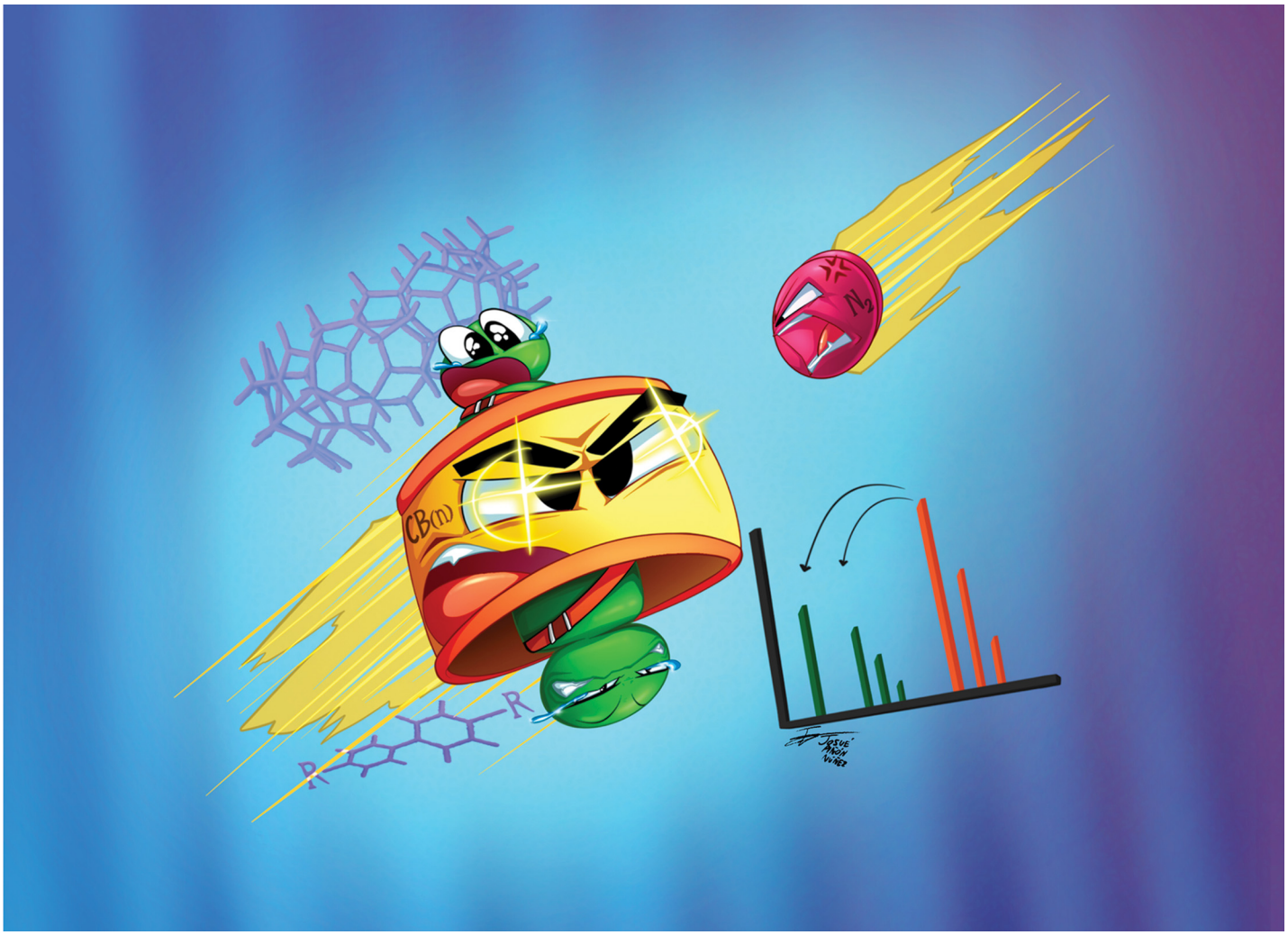

Showcasing research from Prof. J. Laskin lab at Purdue University (USA).

Role of viologen substituents and host size in the gas-phase fragmentation of cucurbituril–viologen host–guest complexes

Gas phase fragmentation of host–guest complexes formed between doubly substituted viologens and cucurbituril is strongly influenced by the size of the host and by the substituents on the viologen guests. Two competitive fragmentation pathways were observed: dissociation by released the charged reduced guest and loss of viologen substituent from the doubly charged complex. Surprisingly, release of doubly charged guest was not observed, which highlights the strong influence of the ion-dipole interactions in these host–guest complexes.

Image reproduced by permission of Julia Laskin from *Phys. Chem. Chem. Phys.*, 2025, **27**, 24713.

Image designed by Josué Piñón Núñez

As featured in:

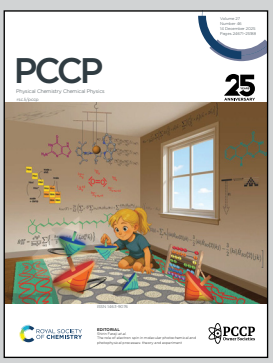

See Julia Laskin *et al.*, *Phys. Chem. Chem. Phys.*, 2025, **27**, 24713.

ROYAL SOCIETY OF CHEMISTRY

rsc.li/pccp

Registered charity number: 207890

PCCP Owner Societies

PCCP

ROYAL SOCIETY OF CHEMISTRY

PAPER

View Article Online
View Journal | View Issue

Cite this: *Phys. Chem. Chem. Phys.*, 2025, **27**, 24713

Role of viologen substituents and host size in the gas-phase fragmentation of cucurbituril–viologen host–guest complexes

Hugo Y. Samayoa-Oviedo, Daniel M. Hristov, Bethany A. Phillips and Julia Laskin *

Viologens are widely used in the development and fabrication of electrochromic devices. One strategy to enhance their stability in solution upon electrochemical reduction is to incorporate them within the cavity of an appropriate host molecule. In solution, the formation of host–viologen complexes is primarily driven by hydrophobic interactions and the displacement of water molecules from the host cavity. Studying these complexes in the gas phase provides insights into the intrinsic factors determining their stability towards fragmentation in the absence of solvent molecules. In this work, we used collision induced dissociation (CID) to assess the relative stability of host–guest complexes formed between cucurbiturils (CBs) and viologen dications. Methyl-, heptyl-, and benzyl-disubstituted viologens were selected as guest species to investigate how alkyl substituents of viologen guests influence the stability of host–guest complexes. Because these complexes are stabilized by ion–dipole interactions, the release of the doubly charged guest is not a preferred fragmentation pathway. Instead, fragmentation occurs *via* either the release of a charge-reduced guest or the loss of neutral substituents. Substituent loss is primarily observed for viologen guests with bulky substituents that extend beyond the host cavity. Meanwhile, the release of a charge reduced guest is a competing pathway for complexes with benzyl or methyl viologen and for complexes in which the guest is not fully encapsulated within the host. We also examined the effect of host size on the strength of host–guest interactions. Our results indicate that the number of effective ion–dipole interactions between the host and the guest is a key factor determining the stability of the complex. Specifically, CB(7) forms the most stable complexes, while complexes with CB(6) exhibit lower stability because the smaller CB(6) host cannot fully accommodate the guest. Meanwhile, the effectiveness of ion–dipole interactions is diminished for CB(8) due to its large cavity size. Overall, this study provides insights into the intrinsic factors, such as host size and guest substitution, that determine the stability of cucurbituril–viologen host–guest complexes towards gas phase fragmentation.

Received 7th August 2025,
Accepted 13th October 2025

DOI: 10.1039/d5cp03029c

rsc.li/pccp

Introduction

Viologens are species composed of a bipyridinium core with one or two side alkyl chains that change color depending on their charge state. Because both their optical and redox properties may be tailored by varying the alkyl chain, counterion, and solvent, viologens are attractive building blocks for the design of functional materials with tunable properties[1–3] and the preparation of electrochromic devices.[4,5] However, fully and partially reduced viologens, especially those with long alkyl chains, suffer from poor solubility in water, which limits their use in functional materials.[6–8] Host–guest chemistry has been previously used to increase the stability[9–11] and solubility[12] of a guest molecule by its incorporation inside an appropriate host. The incorporation of viologens into cucurbiturils (CBs)[13] as host molecules has been used to increase their stability and electrochemical performance in aqueous solutions.[6,14–16] The presence of electron-rich carbonyl groups at the portals of the CB cavity generates a negative quadrupolar field, which stabilizes positively charged viologens *via* ion–dipole interactions.[17–23] The magnitude of the quadrupole moment, which increases with increasing CB size,[24–27] may influence the strength of host–guest interactions. Meanwhile, the hydrophobic cavity of CBs provides a favorable environment for both partially and fully reduced viologens.[14,28,29]

The stability of host–guest complexes has been characterized using a broad range of analytical techniques.[6,22,30–34] Among these techniques, mass spectrometry (MS) provides a unique perspective on the stability of host–guest complexes in

James Tarpo Jr. and Margaret Tarpo Department of Chemistry, Purdue University, West Lafayette, IN 47907, USA. E-mail: jlaskin@purdue.edu; Tel: +1 765-494-5464

the absence of counterions or solvent molecules. Using electrospray ionization (ESI), intact complexes are transferred into the gas phase[35] and their stability towards fragmentation is examined using collision-induced dissociation (CID)[36–39] or other ion activation techniques.[31,40–44] Furthermore, an investigation of the fragmentation pathways of host–guest complexes in the gas phase provides insights into the interactions between the host and the guest.[45,46] For example, in systems where azoalkanes serve as guests, the size of the host determines whether the azoalkanes dissociate from the complex or undergo retro Diels Alder reaction inside the host cavity.[47] In addition, ion–molecule reactions of host–guest complex ions in the gas phase have been used to study their chemical reactivity.[48,49] By studying ion–molecule reactions of crown ether ions in an ion trap, Winkler *et.al.* showed that they catalyze the conversion of propylamine into propene and ammonia.[50] Meanwhile, ion mobility spectrometry has been used to study the conformation[38,51,52] and size[53,54] of supramolecular complexes providing insights into their chemical properties both in the gas and condensed phases.

In this study, we investigated the fragmentation pathways and stability of selected host–guest complexes of CBs and viologens. Specifically, we examined complexes of CB(6), CB(7), and CB(8) with methyl, heptyl, and benzyl viologen (structures shown in Scheme 1) to assess how host size and alkyl substituents of the guest influence preferred fragmentation pathways of the complex. The fragmentation of CB–viologen does not release the doubly charged guest, instead dissociation of the complex occurs through release of charge reduced guests and substituent loss from the complex. The reduction of the guest is facilitated by the negative quadrupole moment of the CB host produced by a network of oxygen atoms at the portals of its cavity.[24–27] Meanwhile, substituent loss is observed for guests containing long substituents that extend beyond the protective cavity of the host. In addition, the fragmentation of the host–guest complexes may involve proton transfer, hydride abstraction, and reduction depending on the individual properties of both the guest and the host. Collision energy-resolved CID experiments provide insights into the effect of the host size on the relative stability of the complex towards fragmentation. We demonstrate that the cavity of CB(6) is too small to fully accommodate viologens with larger alkyl chains, resulting in half-inclusion complexes, which readily fragment in the gas phase. In contrast, the larger cavity sizes of CB(7) and CB(8) promote the formation of stable inclusion complexes with viologen. Notably, because of the optimal size match between host and guest, which maximizes ion–dipole interactions, complexes with CB(7) exhibit the highest gas phase stability towards fragmentation. Overall, our findings offer insights into the factors that stabilize CB–viologen complexes and highlight unique gas-phase ion chemistry arising from host–guest interactions.

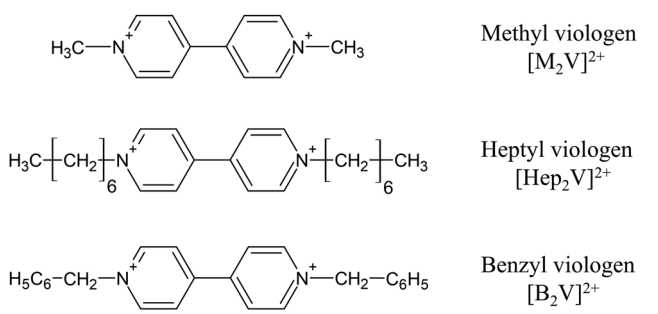

Scheme 1 Structures of the doubly substituted viologens studied in this work.

Experimental section

Chemicals

Cucurbiturils 6, 7, and 8 (all hydrates), benzyl viologen dichloride (B_2VCl_2), methyl viologen dichloride hydrate (M_2VCl_2), and 1,1′-diheptyl-4,4′-bipyridinium dibromide (heptyl viologen dibromide, Hep_2VBr_2) were purchased from Millipore Sigma (St. Louis, MO). Sodium chloride was purchased from Fisher Chemical (Fair Lawn, NJ). 1 mM stock solutions of each individual viologen species were dissolved in DI water. 1 mM cucurbiturils were prepared in 1 mM aqueous NaCl and stirred to promote dissolution. Host–guest complexes were formed by mixing the individual host and guest solutions in a 1 : 1 molar ratio and adding water to obtain a 40 μM concentration of each solution.

Instrumentation

Mass spectrometry and collision energy-resolved CID were performed using an Agilent 6560 ion mobility quadrupole time of flight (IM-QTOF) mass spectrometer (Santa Clara, CA) equipped with a custom-designed ESI source.[55] A syringe pump (KD Scientific, Holliston, MA) was used to propel samples from a 1 mL Hamilton syringe (Reno, NV) through a 150 μm O.D. and 25 μm I.D. fused silica capillary (Polymicro Technologies, Phoenix, AZ) at a flow rate of 0.2–1.0 μL min^{-1}. The capillary was positioned at the mass spectrometer inlet and ESI was performed by applying −4 kV to the entrance of the glass capillary. We used gas temperature of the ion source of 325 °C, fragmentor voltage of 400 V, and octupole RF of 750 V. Data acquisition and analysis was performed using the Agilent Qualitative Navigator software and ChemCalc online tool.[56]

Collision energy-resolved CID of CB–viologen host–guest complexes

To gain insights into the gas phase fragmentation of CB–viologen complexes and facilitate comparisons between complexes containing different hosts, we conducted collision energy-resolved CID experiments. To compare the relative stability of the CB–viologen complexes towards fragmentation we normalized the collision energy to the number of vibrational degrees of freedom of each complex. This approach compensates for the effect of the kinetic shift on the amount of energy required to observe fragmentation of each precursor ion.[57,58] The excitation energy is calculated using eqn (1):

$$\text{Excitation energy} = \frac{\text{C.E.} \times z}{3N - 6} \quad (1)$$

where C.E. is the collision energy in the vendor's arbitrary units, z is the charge state of the ion, and N is the number of atoms in the host–guest complex.

Theoretical calculations

Geometry optimizations of CBs were performed using DFT calculations in the Gaussian 16 program.[59] Previously reported structures were used as the initial geometries.[26] Calculations were performed at the B3LYP level of theory using the 6-31g(d,p) basis set for closed shell systems.[60] Vibrational frequency calculations were performed to confirm that the structures correspond to global energy minima. Proton affinities were calculated using approaches reported in literature.[60]

Results and discussion

In this work, we explore gas phase fragmentation of host–guest complexes of CB with doubly charged viologens. Using collision energy-resolved CID, we examine how host size and alkyl substituent affect the stability of these dications. Specifically, we examine the relative stability and fragmentation pathways of complexes formed between methyl, benzyl, and heptyl viologens with CB(6), CB(7), and CB(8) hosts. The formation of CB–viologen complexes in solution has been previously explored[1–4,6,18,22,61] and these complexes have been also successfully transferred into the gas phase using ESI.[62] Consistent with previous studies, we observed abundant signals corresponding to intact CB–viologen complexes in the ESI-MS spectra of the respective solutions. Mass spectra obtained for all the complexes are shown in Fig. S1, with assignments listed in Table S1. A zoom-in view of the mass spectra in Fig. S1 showing both the experimentally measured and calculated isotopic patterns of the complexes is shown in Fig. S2. Fig. S3 contains the mass spectra with extended m/z ranges of singly charged [CB(n) + M_2V] complexes. CID of the complexes reveals that their fragmentation pathways are largely determined by the properties of the guest, while the competition between pathways is influenced by the host size. To facilitate the discussion, we present the results obtained for each guest separately and conclude with a comparison highlighting key similarities and differences between host–guest complexes with different guests. We first introduce the CID spectrum of a viologen complex with CB(7) and compare it with low-energy fragmentation of the doubly charged viologen guest observed in the MS^2 spectrum obtained at 0 eV collision energy referred to as "isolation spectrum". This is followed by a comparison of the fragmentation efficiency curves obtained using collision energy-resolved CID of the viologen guest with three hosts: CB(6), CB(7), and CB(8), which illustrate the effect of host size on the preferred fragmentation pathway of the complexes.

Fragmentation of CB-methyl viologen complexes

Fragmentation spectra of $[CB(7) + M_2V]^{2+}$ and $[M_2V]^{2+}$ along with the proposed fragmentation pathways of the complex are shown in Fig. 1. The CID spectrum of $[CB(7) + M_2V]^{2+}$ shown in

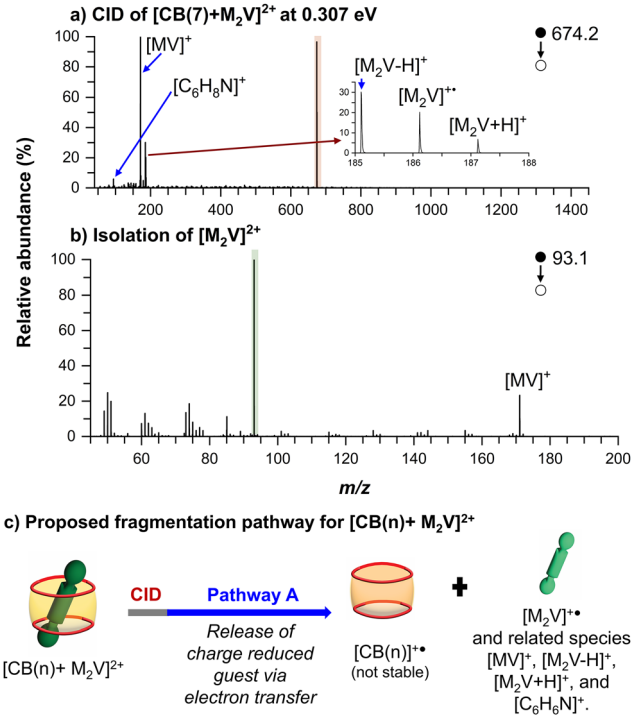

Fig. 1 (a) CID spectrum of $[CB(7) + M_2V]^{2+}$ (m/z 674.2) at 0.307 eV excitation energy, (b) Fragmentation of $[M_2V]^{2+}$ (m/z 93.1) during the isolation step in a mass spectrometer (isolation spectra at 0 eV), and (c) scheme showing the proposed fragmentation pathway of $[CB(7) + M_2V]^{2+}$. In panels a and b precursor m/z are highlighted with colored bars. In panel c the neutral CB host is shown in yellow, while the charged host is shown in orange.

Fig. 1(a) contains singly charged fragment ions of methyl viologen, including $[C_6H_8N]^+$, $[MV]^+$, $[M_2V - H]^+$, $[M_2V]^{+\bullet}$, and $[M_2V + H]^+$. The zoomed-in region of the spectrum shows the $[M_2V - H]^+$, $[M_2V]^{+\bullet}$, and $[M_2V + H]^+$ fragments, which are spaced by 1.007 Da, confirming that these ions are not due to ^{13}C isotopes but instead represent different chemical species. These species were previously observed[62] in the ESI mass spectrum of $[M_2V]^{2+}$ and, along with $[MV]^+$, are formed through the reduction of $[M_2V]^{2+}$ in ESI. Notably, these ions are not observed in the isolation spectrum of $[M_2V]^{2+}$ shown in Fig. 1(b), which instead contains an abundant $[MV]^+$ fragment ion along with several minor fragment ions observed at $m/z < 100$. The presence of an abundant $[M_2V]^{2+}$ peak in Fig. 1(b) indicates that the doubly charged methyl viologen guest is relatively stable in the gas phase. If the fragmentation of $[CB(7) + M_2V]^{2+}$ involved the release of the doubly charged $[M_2V]^{2+}$, followed by its dissociation in the gas phase due to Coulomb repulsion, the resulting mass spectrum in Fig. 1(a) would be expected to resemble the isolation spectrum of $[M_2V]^{2+}$ shown in Fig. 1(b). The absence of $[M_2V]^{2+}$ in Fig. 1(a), along with the presence of ions $[C_6H_8N]^+$, $[M_2V - H]^+$, $[M_2V]^{+\bullet}$, and $[M_2V + H]^+$ ions absent in Fig. 1(b) suggests that the ejection of the doubly charged viologen is not a dominant fragmentation pathway of $[CB(7) + M_2V]^{2+}$. In addition, the isolation spectrum of $[M_2V]^{+\bullet}$ in Fig. S4 contains $[MV]^+$ as

a product, indicating that the $[MV]^+$ observed in Fig. 1(a) can arise from spontaneous fragmentation of $[M_2V]^{+\bullet}$.

The presence of singly charged fragments of methyl viologen in the CID spectrum of $[CB(7) + M_2V]^{2+}$ indicates that the guest undergoes simultaneous reduction and decomposition as it exits the CB cavity, in a process analogous to the one observed in the ESI mass spectrum of the guest.[62] In the proposed fragmentation pathway shown in Fig. 1(c), we refer to this process as pathway A. This pathway involves the reduction of $[M_2V]^{2+}$ through electron transfer from the host, facilitated by the high electron density at the CB portals.[20–22,24,26] Fragmentation of $[CB(7) + M_2V]^{2+}$ *via* pathway A is expected to produce $[CB(7)]^{+\bullet}$ as a complementary fragment ion. The absence of $[CB(7)]^{+\bullet}$ in the CID spectrum of $[CB(7) + M_2V]^{2+}$ can be attributed to the low stability of this radical cation and its rapid dissociation in the gas phase. Indeed, we observe numerous low-abundance ions with $m/z < 673$, which likely correspond to fragments of $[CB(7)]^{+\bullet}$. A zoom-in region of Fig. 1(a) showing these fragments is provided in Fig. S5, with mass assignments listed in Table S2.

The fragmentation efficiency curves of complexes containing methyl viologen, shown in Fig. 2, provide insights into the effect of host size on their fragmentation. Fig. 2(a) presents a comparison of the fragmentation efficiency curves of $[MV]^+$, the major fragment ion produced from all three CB complexes with methyl viologen. The yield of this fragment is similar for all three precursors, whereas the energy threshold varies with the size of the host. Specifically, the energy threshold for the formation of $[MV]^+$ increases in the order: CB(6) < CB(8) < CB(7), reflecting the relative strength of host–guest interactions within each complex. Previous studies indicate that the negative quadrupole moment of CBs increases with CB size.[24–27] While an increased negative quadrupole moment results in a higher magnitude of the ion–dipole interaction of CB–methyl viologen, the stability trend in Fig. 2(a) suggests that there are other factors beyond ion–dipole interactions that affect the stability of these complexes, as discussed later in the text.

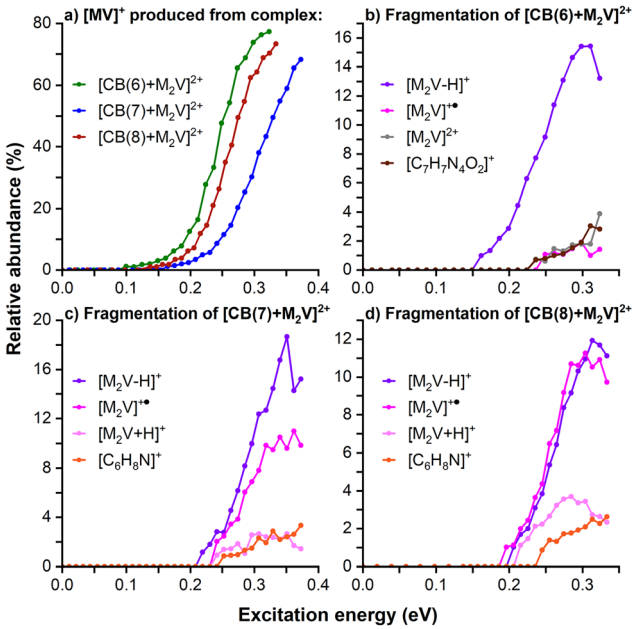

Fig. 2 Fragmentation efficiency curves of the (a) $[MV]^+$ fragment produced from different precursors and other fragment ions of (b) $[CB(6) + M_2V]^{2+}$, (c) $[CB(7) + M_2V]^{2+}$, and (d) $[CB(8) + M_2V]^{2+}$ complexes.

In addition to $[MV]^+$, CID of CB–methyl viologen complexes produces several less abundant fragment ions. Fragmentation efficiency curves of the minor fragments of $[CB(6) + M_2V]^{2+}$ are shown in Fig. 2(b). A product corresponding to the net loss of a hydrogen atom from methyl viologen radical cation, $[M_2V - H]^+$, is formed at 0.16 eV excitation energy, which is 0.05 eV higher than the threshold for the formation of $[MV]^+$. We hypothesize that $[M_2V - H]^+$ is generated *via* pathway A, where the reduced $[M_2V]^{+\bullet}$ species undergoes hydrogen atom loss.[62] Additionally, three low-abundance fragments: $[M_2V]^{+\bullet}$, $[C_7H_7N_4O_2]^+$, and $[M_2V]^{2+}$, are observed at excitation energies above 0.24 eV. The presence of $[M_2V]^{+\bullet}$ in the mass spectrum supports the hypothesis that the guest is reduced by the host within the complex. As discussed earlier, its complementary fragment, $[CB(6)]^{+\bullet}$ is unstable and dissociates into multiple low m/z products. The $[C_7H_7N_4O_2]^+$ fragment ion, is one of the low-abundance fragments of the unstable $[CB(6)]^{+\bullet}$ species shown in Fig. S5 and listed in Table S2. This fragment corresponds to the CB(6) subunit containing one additional methylene group. The formation of the low-abundance $[M_2V]^{2+}$ fragment, which is only observed for the smallest CB(6) host at high excitation energies, may be indicative of an entropically favorable pathway that becomes accessible at higher internal energies. This pathway likely proceeds through the ejection of the doubly charged guest previously reported for cyclodextrin-based complexes.[37] The absence of this product in CID spectra of complexes with CB(7) and CB(8) shown in Fig. 2(c) and (d), respectively, indicates that $[M_2V]^{2+}$ is not fully accommodated inside the CB(6) cavity and forms a half-inclusion complex. In contrast, the larger cavities of CB(7) and CB(8) can fully encapsulate $[M_2V]^{2+}$, which hinders the ejection of the doubly charged guest. Half-inclusion complexes have been experimentally observed and computationally modeled for small hosts or large guests.[20,22]

The relative abundance of $[M_2V]^{+\bullet}$ increases with increasing host size, suggesting that larger hosts facilitate the reduction of $[M_2V]^{2+}$. It is reasonable to assume that the larger and more delocalized quadrupole electric field generated by larger hosts,[24–27] enhances the reduction yield of $[M_2V]^{2+}$ to $[M_2V]^{+\bullet}$, thereby increasing the abundance of reduced fragments. Specifically, a comparison of Fig. 2(c) and (d) reveals that the relative abundance of $[M_2V - H]^+$ decreases while the relative abundance of $[M_2V + H]^+$ increases with host size. In addition, CID of complexes with CB(7) and CB(8) generates methylpyridinium fragment ion, $[C_6H_8N]^+$, a product of $[M_2V]^{+\bullet}$, which appears at higher excitation energies above 0.25 eV. The absence of this product in the CID of $[CB(6) + M_2V]^{2+}$ may be attributed to the low yield of the reduced $[M_2V]^{+\bullet}$ species in the gas-phase fragmentation of this precursor ion.

Overall, the results shown in Fig. 2 indicate that pathway A is the dominant fragmentation pathway for CB complexes with

methyl viologen, suggesting that dissociation primarily proceeds through the release of a charge-reduced guest. The reduction proceeds through electron transfer to the host, generating the radical cation of methyl viologen, $[M_2V]^{+\bullet}$ and other species formed from its decomposition. As the size of the host increases, the yield of the $[M_2V]^{+\bullet}$ fragment also increases, which we attribute to the higher negative quadrupole moment of larger CB hosts, leading to more efficient electron transfer. The results in Fig. 2(a) also indicate that the overall strength of the host–guest complex increases in the order: CB(6) < CB(8) < CB(7), which will be further discussed later in the text.

Fragmentation of CB–heptyl viologen complexes

Fragmentation spectra of $[CB(7) + Hep_2V]^{2+}$ and $[Hep_2V]^{2+}$ along with the proposed fragmentation pathways of the complexes with all the hosts are shown in Fig. 3. The CID spectrum of $[CB(7) + Hep_2V]^{2+}$ shown in Fig. 3(a) reveals a distinct fragmentation pattern, containing singly charged fragment ions $[C_4H_9]^+$, $[V + H]^+$, $[HepV]^+$, and $[CB(7) + H]^+$. The mass spectrum also contains doubly charged $[CB(7) + V + 2H]^{2+}$ and $[CB(7) + HepV + H]^{2+}$ ions corresponding to one and two losses of C_7H_{14} from $[CB(7) + Hep_2V]^{2+}$, respectively. When comparing the CID spectrum of $[CB(7) + Hep_2V]^{2+}$ (Fig. 3(a)) with that of $[CB(7) + M_2V]^{2+}$ (Fig. 2(a)), we observed three key differences that indicate that fragmentation of $[CB(7) + Hep_2V]^{2+}$ does not involve pathway A. First, the CID spectrum of $[CB(7) + Hep_2V]^{2+}$ contains $[CB(7) + H]^+$ which indicates that the fragmentation of the complex results in proton transfer to the host. Second, the spectrum of $[CB(7) + Hep_2V]^{2+}$ in Fig. 3(a) contains abundant doubly charged fragment ions in which the guest is retained inside the host. Finally, the CID spectrum in Fig. 3(a) does not contain fragment ions resulting from electron transfer to the guest, *i.e.* $[Hep_2V]^{+\bullet}$. Furthermore, a comparison of the CID spectrum of $[CB(7) + Hep_2V]^{2+}$ in Fig. 3(a) with the isolation spectrum of $[Hep_2V]^{2+}$ in Fig. 3(b) indicates that the release of doubly charged guest does not occur in dissociation of $[CB(7) + Hep_2V]^{2+}$. Specifically, if $[Hep_2V]^{2+}$ were produced from fragmentation of $[CB(7) + Hep_2V]^{2+}$, it should appear in Fig. 3(a), given that $[Hep_2V]^{2+}$ is a relatively stable species in the gas phase as shown in Fig. 3(b).

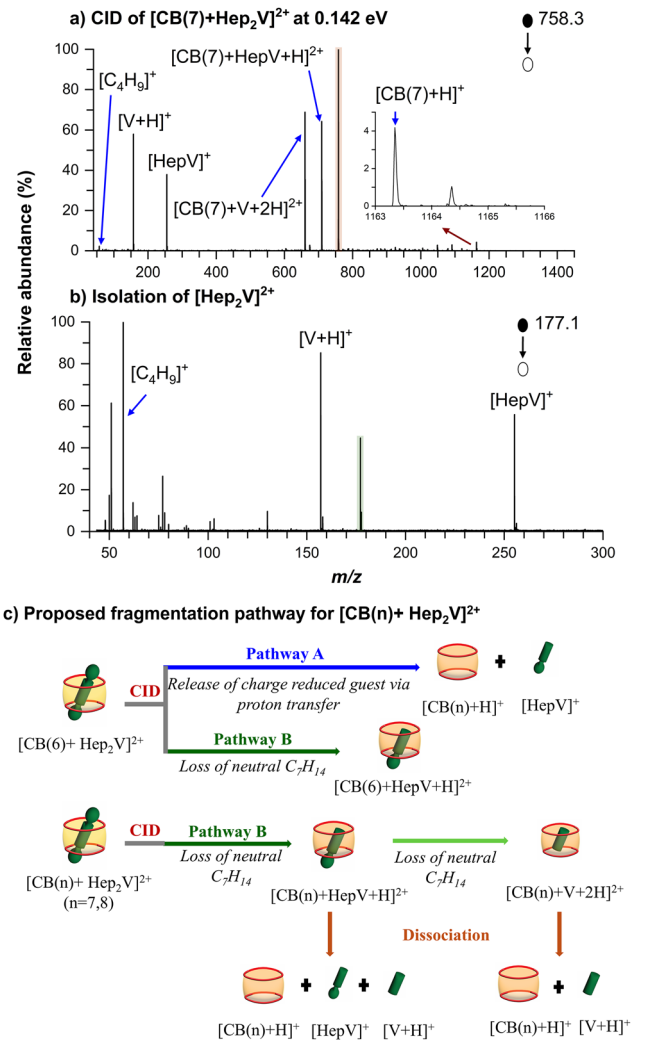

Fig. 3 (a) CID spectrum of $[CB(7) + Hep_2V]^{2+}$ (*m*/*z* 758.3) at 0.142 eV excitation energy, (b) fragmentation of $[Hep_2V]^{2+}$ (*m*/*z* 177.1) during the isolation step in a mass spectrometer (isolation spectra at 0 eV), and (c) scheme showing the proposed fragmentation pathway of $[CB(7) + Hep_2V]^{2+}$ complexes. In panels a and b precursor *m*/*z* are highlighted in colored bars. In panel c the neutral CB host is shown in yellow, while the charged host is shown in orange.

The presence of abundant $[CB(7) + V + 2H]^{2+}$ and $[CB(7) + HepV + H]^{2+}$ ions in Fig. 3(a), indicates that the loss of alkyl chains from the complex is a major fragmentation pathway of $[CB(7) + Hep_2V]^{2+}$. In this pathway (pathway B in Fig. 3(c)), an alkyl chain is lost as a neutral species with the chemical formula C_7H_{14}. The loss of neutral alkyl chain is accompanied by proton transfer from the leaving group to the complex, resulting in the formation of $[CB(7) + HepV + H]^{2+}$ which undergoes a sequential fragmentation step forming $[CB(7) + V + 2H]^+$. Loss of heptyl chains from heptyl viologen should produce $[C_4H_9]^+$ as shown in the isolation spectrum of $[Hep_2V]^{2+}$ in Fig. 3(b). $[C_4H_9]^+$ is a product of the decomposition of the heptyl cation[63–68] and is the complementary species to $[V + H]^+$ and $[HepV]^+$. Although $[C_4H_9]^+$ is a major species in Fig. 3(b), it is practically absent in Fig. 3(a). We suggest that during fragmentation of $[CB(7) + Hep_2V]^{2+}$ proton transfer to the host competes with the formation of $[C_4H_9]^+$. Theoretical calculations of gas phase proton affinities of CBs, based on their optimized electronic structures and the methodology described in the experimental section, yield values of 1041, 1029, and 1020 kJ mol^{-1} for CB(6), CB(7), and CB(8), respectively. In comparison, the reported proton affinities for isobutene and *trans*-2-butene, the neutral counterparts of the cationic products of the heptyl cation decomposition,[63–68] are significantly lower, at 823.4 and 773.6 kkJ mol^{-1}, respectively.[67] This indicates that CBs can efficiently compete for proton[69] with the heptyl cation during the fragmentation of $[CB(n) + Hep_2V]^{2+}$ complexes.

We suggest that the singly charged $[V + H]^+$, $[HepV]^+$, and $[CB(7) + H]^+$ species observed in Fig. 3(a) are products of sequential fragmentation of either $[CB(7) + V + 2H]^{2+}$ or $[CB(7) + HepV + H]^{2+}$. We analyzed the fragmentation efficiency

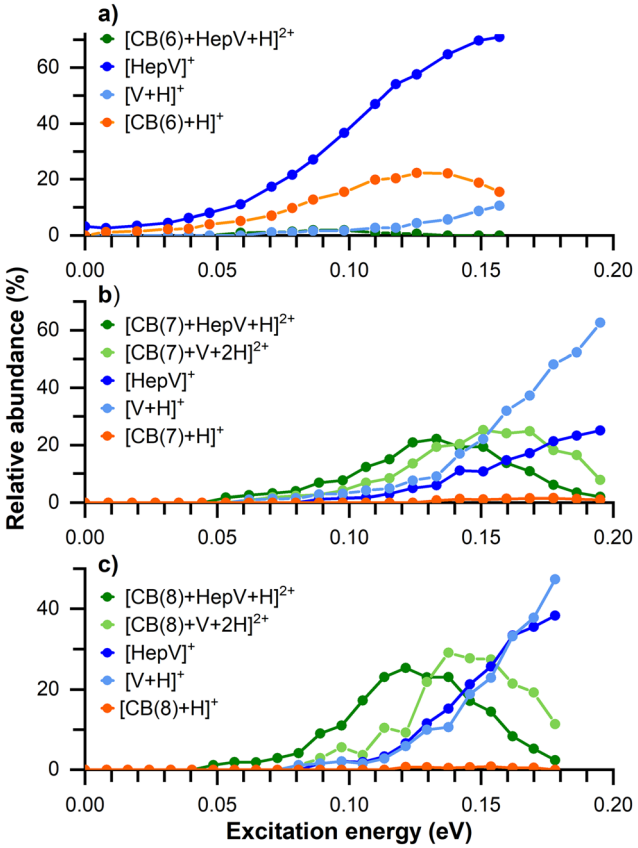

Fig. 4 Fragmentation efficiency curves of (a) $[CB(6) + Hep_2V]^{2+}$, (b) $[CB(7) + Hep_2V]^{2+}$, and (c) $[CB(8) + Hep_2V]^{2+}$.

curves of the complexes shown in Fig. 4 to confirm this assertion. We observe that the fragmentation efficiency curves of complexes with CB(7) and CB(8) (Fig. 4(b) and (c), respectively) are similar to each other, yet notably different from those of the CB(6) complex shown in Fig. 4(a). Specifically, Fig. 4(b) and (c) show that the lowest energy fragmentation of $[CB(7) + Hep_2V]^{2+}$ and $[CB(8) + Hep_2V]^{2+}$ occurs *via* pathway B, which becomes accessible at ~0.05 eV excitation energy. The major low-energy fragment, $[CB(n) + HepV + H]^+$, formed through the loss of one heptyl substituent, undergoes the loss of an additional heptyl chain at higher excitation energies, resulting in the formation of the $[CB(n) + V + 2H]^+$ fragment ion. In contrast, the fragmentation curves of $[CB(6) + Hep_2V]^{2+}$ in Fig. 4(a) indicate that $[HepV]^+$ is the major low-energy fragment of this complex, while, $[HepV]^+$ and $[V + H]^+$ in Fig. 4(b) and (c) are only observed at substantially higher collision energies as secondary products of $[CB(7,8) + V + 2H]^{2+}$ or $[CB(7,8) + HepV + H]^{2+}$. This observation indicates that $[HepV]^+$ and $[V + H]^+$ are not produced directly from $[CB(7,8) + Hep_2V]^{2+}$. The MS^3 spectrum of $[CB(7) + HepV + H]^{2+}$ shown in Fig. S6 corroborates that $[V + H]^+$ and $[HepV]^+$ are instead the products of $[CB(7) + HepV + H]^{2+}$ formed probably through Coulomb fission.

The fragmentation efficiency curve of $[CB(6) + Hep_2V]^{2+}$ in Fig. 4(a) indicates its low gas phase stability with considerable fragmentation occurring even during isolation in the collision cell. At lower excitation energies, the fragmentation of $[CB(6) + Hep_2V]^{2+}$ produces $[HepV]^+$ and $[CB(6) + H]^+$. This pathway involving the release of charge reduced guest with proton transfer to the host (pathway A in Fig. 3(c)) is not observed for complexes with CB(7) and CB(8) hosts, indicating structural differences between $[CB(6) + Hep_2V]^{2+}$ and its CB(7) and CB(8) analogs. It is reasonable to assume that in $[CB(6) + Hep_2V]^{2+}$, the guest is only partially incorporated into the CB(6) host, forming a half-inclusion complex similar to the one previously observed in solution.[22] Such complexes readily release the guest. Meanwhile, a small fraction of $[CB(6) + Hep_2V]^{2+}$ ions that undergo fragmentation *via* pathway B at higher excitation energies between 0.05 and 0.13 eV likely correspond to inclusion complexes that exhibit stronger binding of the guest. For $[CB(n) + Hep_2V]^{2+}$ complexes, the loss of alkyl substituents through pathway B is facilitated by the long alkyl chains extruding from the cavity of the host. Consequently, the threshold excitation energy for the observation of products from pathway B should be largely independent of the host size. Indeed, Fig. 4 shows that, for all three precursors, the first loss of the neutral alkyl chain is observed at the same excitation energy of ~0.05 eV. Moreover, the relative abundances and appearance energies of $[CB(n) + HepV + H]^{2+}$ are almost identical for the inclusion complexes of CB(7) and CB(8).

Another striking observation from the fragmentation efficiency curves in Fig. 4 is the decrease in the relative abundance of the protonated host, shown as an orange trace, with increasing host size. In Fig. 4(a), the relative abundance of $[CB(6) + H]^+$ reaches 25% at the excitation energy of 0.13 eV, highlighting the importance of pathway A in the fragmentation of $[CB(6) + Hep_2V]^{2+}$. In contrast, the relative abundance of $[CB(7) + H]^+$ and $[CB(8) + H]^+$ remain below 3% across all excitation energies. This trend may be attributed to increased scattering at higher excitation energies where pathway A occurs, as well as to the lower proton affinity and increased delocalization of the electric quadrupole in the larger CBs,[24–27] which collectively reduce the stability of the protonated host in the gas phase.

Overall, the results presented in Fig. 3 and 4 indicate that pathway B, involving the loss of neutral C_7H_{14}, is the predominant fragmentation channel for $[CB(7) + Hep_2V]^{2+}$ and $[CB(8) + Hep_2V]^{2+}$ complexes. It is reasonable to assume that the long alkyl chains of the guest extend outside of the protecting cavity of the host, making them more susceptible to fragmentation. In contrast, $[(CB6) + Hep_2V]^{2+}$ adopts a half-inclusion conformation in the gas phase and its fragmentation follows predominantly pathway A, involving proton transfer to the host and the release of charge-reduced guest.

Fragmentation of CB–benzyl viologen complexes

Fragmentation spectra of $[CB(7) + B_2V]^{2+}$ and $[B_2V]^{2+}$ along with the proposed fragmentation pathway of the complexes with all the hosts are shown in Fig. 5. The CID spectrum of $[CB(7) + B_2V]^{2+}$ in Fig. 5(a) contains singly charged fragment ions, $[B]^+$ and $[BV]^+$, in the low *m*/*z* range, along with

$[CB(7) - H]^+$ and $[CB(7) + BV]^+$ ions in the high *m/z* range. While ions $[B]^+$ and $[BV]^+$ may initially appear as complementary species formed through gas phase fission of $[B_2V]^{2+}$, the absence of $[BV]^+$ in the isolation spectrum of $[B_2V]^{2+}$ (Fig. 5(b)) suggests an alternative fragmentation pathway. We note that the precursor ion, $[B_2V]^{2+}$, is absent in Fig. 5(b), indicating its low stability towards gas phase fragmentation. This is consistent with its low abundance in the ESI mass spectrum shown in Fig. S7. The low stability of $[B_2V]^{2+}$ may be attributed to both its facile reduction during ESI[62] and Coulomb repulsion under vacuum. Despite the low abundance of $[B_2V]^{2+}$, we were able to acquire its isolation spectrum by averaging 162 individual scans. Fig. 5(b) shows that the fragmentation of $[B_2V]^{2+}$ in the gas phase releases both benzyl substituents as cations, producing neutral bipyridine ($C_{10}H_8N_2$) as complementary species.

We propose that $[BV]^+$ observed in the MS^2 of $[CB(7) + B_2V]^{2+}$ is generated through pathway A. Unlike complexes with methyl and heptyl viologen, the release of charge-reduced $[B_2V]^{2+}$ is accompanied by hydride abstraction from CB(7). This process produces $[BV]^+$, $[CB(7) - H]^+$, and neutral benzene, with both cations observed in Fig. 5(a). Hydride abstraction has been previously reported in reactions of benzyl cations with electron donating species capable of stabilizing hydride loss.[70,71] In Fig. 5(a), the fragmentation of $[CB(7) + B_2V]^{2+}$ also produces $[B]^+$ and $[CB(7) + BV]^+$, which are likely complementary species formed through the loss of alkyl substituent (pathway B) from $[CB(7) + B_2V]^{2+}$. In contrast with complexes containing heptyl viologen where the substituent is lost as a neutral species after proton transfer to the host, in complexes containing benzyl viologen, the substituent is lost as a benzyl cation. Additionally, the loss of benzyl cation from $[CB(7) + B_2V]^{2+}$ is favorable due to the high gas phase stability of $[B]^+$. These observations highlight the effect of the substituent on the fragmentation of the host guest complexes of substituted viologens.

Fragmentation efficiency curves of CB–benzyl viologen complexes are shown in Fig. 6, where product ions formed through pathway A are marked in purple and pink, while those formed through pathway B are marked in green. Similar to the results obtained for the $[CB(n) + Hep_2V]^{2+}$ precursors, fragmentation efficiency curves for benzyl viologen complexes with CB(7) and CB(8) shown in Fig. 6(b) and (c), respectively, are similar to each other but distinctly different from that of the CB(6) complex (Fig. 6(a)). For example, in CID of $[CB(6) + B_2V]^{2+}$, pathway A (purple and pink traces) occurs at lower excitation energies than pathway B (green traces). In contrast, for complexes with CB(7) and CB(8), pathway B is preferred at lower excitation energies. The $[CB(6) + B_2V]^{2+}$ complex exhibits low gas phase stability, fragmenting at 0.02 eV, while fragmentation of more stable $[CB(7) + B_2V]^{2+}$ and $[CB(8) + B_2V]^{2+}$ precursors is observed at higher excitation energies of 0.07 and 0.09 eV, respectively.

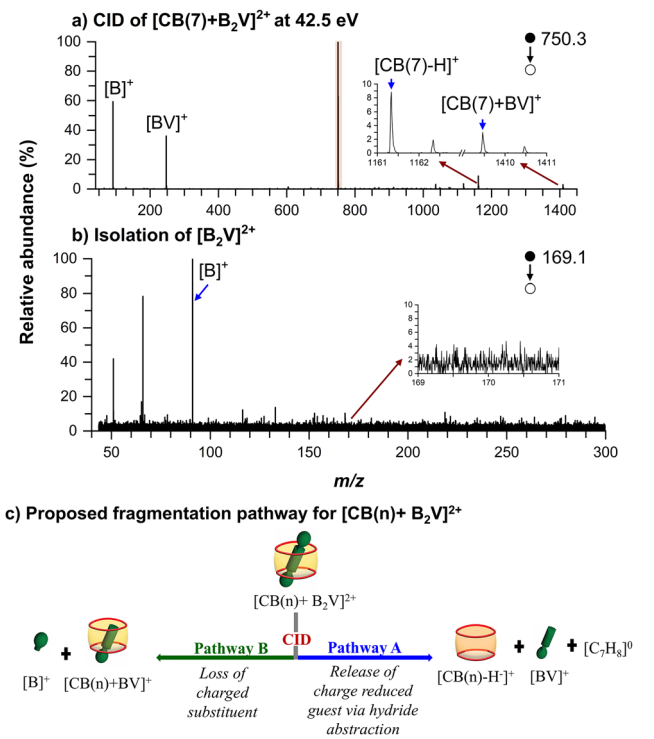

Fig. 5 (a) A 42.5 eV CID spectrum of $[CB(7) + Hep_2V]^{2+}$ (*m/z* 750.3), (b) Fragmentation of $[Hep_2V]^{2+}$ (*m/z* 169.1) during the isolation step in a mass spectrometer (isolation spectra at 0 eV), and (c) Scheme showing the proposed fragmentation pathway of $[CB(7) + B_2V]^{2+}$ complexes. In panel a precursor *m/z* is highlighted in color bar. In panel c the neutral CB host is shown in yellow, while the charged host is shown in orange.

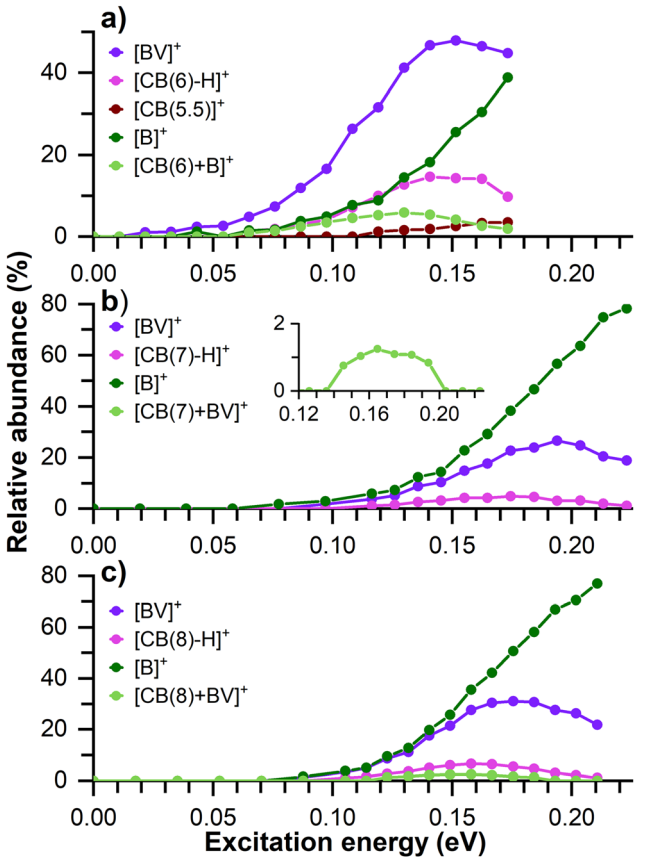

Fig. 6 Fragmentation efficiency curves of (a) $[CB(6) + B_2V]^{2+}$, (b) $[CB(7) + B_2V]^{2+}$, and (c) $[CB(8) + B_2V]^{2+}$.

We propose that, similar to the previously discussed $[CB(6) + Hep_2V]^{2+}$ complex, $[CB(6) + B_2V]^{2+}$ adopts a half-inclusion configuration. Additionally, CID of $[CB(6) + B_2V]^{2+}$ produces distinct product ions compared to $[CB(7) + B_2V]^{2+}$ and $[CB(8) + B_2V]^{2+}$. Notably, $[CB(6) + B]^+$ is a unique product ion observed exclusively in the fragmentation of $[CB(6) + B_2V]^{2+}$. We propose that fragmentation of this complex through pathway B generates $[CB(6) + B]^+$ by eliminating $[BV]^+$. This process is likely facilitated by the half-inclusion conformation of $[CB(6) + B_2V]^{2+}$ where the viologen core is less protected by the CB(6) cavity. The $[C_{33}H_{33}N_{22}O_{11}]^+$ ion is another fragment of $[CB(6) + B_2V]^{2+}$ observed at excitation energies above 0.12 eV. Its chemical formula corresponds to five CB subunits and a $C_3H_3N_2O$ moiety, representing exactly half of a CB subunit. We propose that this fragment ion, labeled as $[CB(5.5)]^+$ in Fig. 6(a) and Table S2, is a secondary product of $[CB(6) - H]^+$. The higher abundance of $[CB(6) - H]^+$ in Fig. 6(a) enables the detection of $[CB(5.5)]^+$ at higher excitation energies.

The fragmentation efficiency curves in Fig. 6 indicate that the release of $[B_2V]^{2+}$ is not an observed fragmentation pathway for the complexes. Specifically, $[CB(7,8) + B_2V]^{2+}$ and $[CB(7,8) + Hep_2V]^{2+}$ exhibit similar threshold excitation energies (~0.08 eV) for pathway B, which involves substituent loss. This similarity suggests that substituent loss is more favorable than release of $[B_2V]^{2+}$ at lower excitation energies.

In summary, host–guest complexes of CB(n) and $[B_2V]^{2+}$ undergo fragmentation *via* both pathways A and B. Pathway A is the predominant pathway for the smaller CB(6) host, which cannot fully accommodate the guest. Notably, pathway A involves hydride transfer from the host to the $[B]^+$ cation forming $[CB(n) - H]^+$ and a neutral toluene fragment.[71] In contrast, complexes with CB(7) and CB(8) preferentially fragment *via* pathway B. Pathway B is attributed to the benzyl substituents extending outside the protective cavity of the host, which facilitates their loss from the complex.

Summary of the observed fragmentation pathways

Collectively, the results of collision energy-resolved CID experiments in Fig. 1–6 indicate that the fragmentation pathways of CB–viologen complexes in the gas phase depend on the identity of the host and guest molecules. We have identified two main pathways for their fragmentation, which are summarized in Scheme 2. In pathway A, a charge reduced guest is released from the host while pathway B involves the loss of a substituent from the CB–viologen complex. Notably, we do not observe evidence for the release of doubly charged viologen guests from the complexes. This may be attributed to strong ion–dipole interactions between the doubly charged viologen and the negatively charged portals of CBs.[20–22,24,26] Dissociation of the complex during CID involves the transfer of the guest through one of the negatively polarized portals of CB[24–27] and results in the release of a charge reduced guest. Additionally, the absence of intact viologen dications among the dissociation products may reflect the inherent instability of these species in the gas phase due to Coulomb repulsion.[72]

Based on the observations from the previous sections, we can draw conclusions about the preferred fragmentation

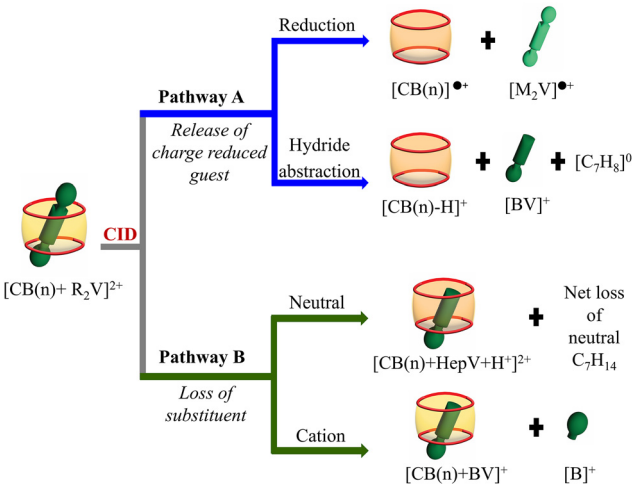

Scheme 2 Fragmentation pathways of CB–viologen complexes. Neutral CB host is shown in yellow, while the charged host is shown in orange. The radical methyl viologen, $[M_2V]^{+\bullet}$, is shown in lighter green to highlight the presence of this species in comparison with other guests that are even electron ions.

pathways for these complexes. Fragmentation of complexes containing guests with long substituents extending outside of the cavity of CB follows pathway B. In this pathway, complexes containing heptyl and benzyl viologen lose the substituent as a neutral and charged species, respectively. The release of charge reduced guest (pathway A) is a competitive pathway to pathway B. Pathway A is the only observed fragmentation pathway for guests with short alkyl substituents, *i.e.* $[M_2V]^{2+}$. In pathway A, $[M_2V]^{2+}$ gets reduced as it leaves the cavity of the host due to the negative electric field at the portals of CBs which increases with host size. Hydride transfer to the guest through pathway A is observed for complexes with benzyl viologen and results in the formation of toluene, $[BV]^+$, and $[CB(n) - H]^+$. Meanwhile, proton transfer through pathway A was observed for $[CB(6) + Hep_2V]^{2+}$ but not for its analogs with CB(7) and CB(8). In addition, the results above highlight the remarkable influence of the host size on the preferred fragmentation pathways of CB–viologen complexes. Complexes with CB(7) and CB(8) fragment through pathway B at lower collision energies, while half-inclusion complexes with CB(6) fragment through pathway A.

Survival yield curves of CB–viologen complexes

The collision energy required to fragment CB–viologen complexes in the gas phase may be used to compare the intrinsic stability of the complexes towards fragmentation in the absence of solvent molecules or counterions. We used collision energy-resolved CID to obtain the survival yield (S_y) of the precursor ion as a function of collision energy. The S_Y represents the relative abundance of the precursor ion normalized to the total signal of the precursor ion and its fragments at a given collision energy. The survival yield curves for all complexes are shown in Fig. 7(a)–(c) and the excitation energies required to achieve 50% fragmentation of each complex ($S_{Y,50\%}$) are summarized in Fig. 7(d). We observe that, for all the guests, complexes

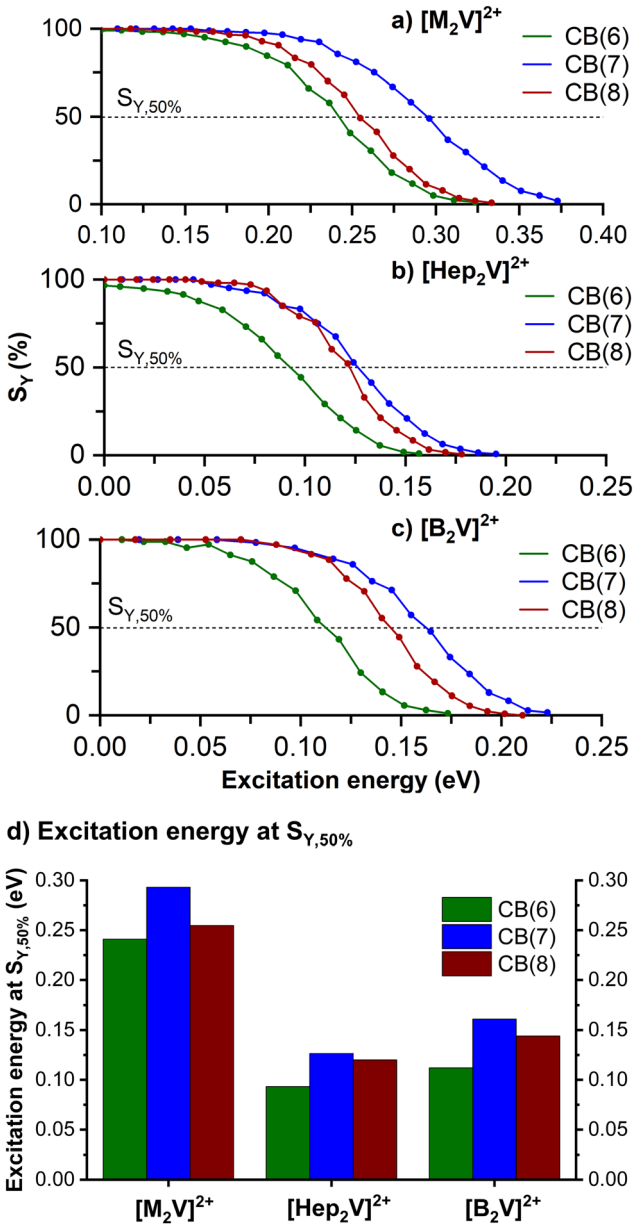

Fig. 7 Survival yield curves of complexes containing (a) methyl viologen, (b) heptyl viologen, and (c) benzyl viologen representing the fraction of intact precursor ions as a function of the excitation energy. (d) Summary of the excitation energies required to achieve 50% fragmentation ($S_{Y,50\%}$) for the CB–viologen host–guest complexes.

of CB(7) are more stable than their CB(6) and CB(8) analogs. Although hosts with larger cavity size are expected to better accommodate the guest and that a larger negative quadrupole moment of the CB cavity can better stabilize doubly charged viologen guests, the relative stability of the complexes does not follow the expected trend with cavity size and quadrupole moment.[24–27] This finding indicates that other factors influence the stability of the CB–viologen host–guest complexes. We propose that the number of effective host–guest interactions plays a dominant role in determining the stability of CB–viologen complexes. These complexes are stabilized by ion–dipole interactions,[13,20,21] which are diminished when the host size is either too small or too large relative to the guest. Our results indicate that CB(7) offers an optimal cavity size that maximizes interactions with viologen guests, thereby enhancing the stability of the host–guest complex. In contrast, the smaller cavity of CB(6) cannot fully accommodate the guest, leading to half-inclusion complexes, which are less stable toward fragmentation than inclusion complexes with CB(7) and CB(8). Additionally, the larger cavity of CB(8) likely results in increased distances between the cationic sites of the guests and the functional groups lining the host cavity, weakening the overall interaction as compared to complexes with CB(7).

Conclusions

The intact transfer of CB–viologen host–guest complexes into the gas phase provides an opportunity to investigate the effect of the host size and the structure of the alkyl substituents of viologen guests on the stability and fragmentation pathways. For complexes containing the same guest, the strength of host–guest interactions is primarily determined by the number of effective ion–dipole interactions between the charged guest and negative cavity of the host, which is influenced by the cavity size. Our results reveal that the optimal fit of viologen guest inside the CB(7) cavity helps maximize its interactions with the oxygen atoms lining the host cavity. As a result, complexes with CB(7) exhibit the highest stability toward fragmentation. In contrast, complexes with CB(6), which predominately assume half-inclusion configuration, exhibit lower stability, while complexes with CB(8) are slightly destabilized compared to their CB(7) analogs because their larger cavity reduces the effectiveness of ion–dipole interactions.

Upon collisional activation, the complexes either undergo dissociation by releasing the charge reduced guest (pathway A) or lose a substituent from the doubly charged complex (pathway B). The strong ion–dipole interaction in these complexes prevents the release of intact doubly charged guest from the host. Fragmentation of complexes with viologens with long alkyl chain substituents, such as heptyl and benzyl viologen, results in pathway B as the preferred low-energy pathway. An alternative fragmentation pathway emerges for complexes with short alkyl chains, such as methyl viologen, in which the reduced guest is released from the host as a consequence of the negative quadrupole electric field of the host. Complexes with benzyl viologen also undergo fragmentation through pathway A with hydride transfer to the guest which results in the formation of toluene and $[BV]^+$ with $[CB(n)–H]^+$ as the complementary ion. The extent to which products from pathway A are observed is influenced by the strength of the negative quadrupole moment of the host. Pathway A was also observed for complexes with CB(6) because of the lower stability in complexes with half-inclusion conformation.

Overall, the study of the fragmentation pathways of CB–viologen complexes indicates that there are other factors beyond ion–dipole interactions that affect their stability towards

fragmentation in the gas phase. Our results provide insights into the intrinsic stability and fragmentation pathways of CB–viologen host guest complexes. This knowledge has broader implications for the design of materials that rely on strong host–guest interactions such as supramolecular assemblies.

Author contributions

Conceptualization: HYSO and JL. Funding acquisition: JL. Methodology: HYSO and JL. Investigation: HYSO, DMH, and BAP. Supervision: HYSO and JL. Validation: HYSO, DMH, BAP, and JL. Visualization: HYSO, DMH, and BAP. Writing – original draft: HYSO. Writing – review & editing: HYSO, DMH, BAP, and JL.

Conflicts of interest

The authors declare that they have no conflict of interest.

Data availability

All data underpinning this work are provided in the supplementary information (SI). Supplementary information: additional information is provided regarding ESI-MS of solutions containing the host–guest complexes and their mass assignments. Isolation spectra of methyl viologen fragment ions. Zoomed in MS^2 of $[CB(7) + M_2V]^{2+}$ at 70 eV and their mass assignments. Fragmentation efficiency curve of $[CB(7) + HepV + H]^{2+}$. ESI-MS of $[B_2V]Cl_2$. CB(n) and $[CB(n) + H]^+$ optimized structures. See DOI: https://doi.org/10.1039/d5cp03029c.

Acknowledgements

Part of this research was supported by the grant FA9550-23-1-0137 from the Air Force Office of Scientific Research (AFOSR) and the grant 2508569 from the National Science Foundation (NSF). DMH thanks the Purdue University Department of Chemistry's undergraduate summer research program, the Purdue Chapter of the American Chemical Society Student Affiliate Club (ACS-SA), and the Purdue University ''Learning Beyond the Classroom'' certificate program, all of which provided funding for conference traveling and summer internships related to this work. Computational experiments were conducted at the Rosen Center for Advanced Computing[73] at Purdue University.

References

1 L. Striepe and T. Baumgartner, Viologens and Their Application as Functional Materials, *Chem. – Eur. J.*, 2017, **23**(67), 16924–16940, DOI: 10.1002/chem.201703348.
2 Y. Dai, Z. Xie, M. Bao, C. Liu and Y. Su, Multiple Stable Redox States and Tunable Ground States *via* the Marriage of Viologens and Chichibabin's Hydrocarbon, *Chem. Sci.*, 2023, **14**(13), 3548–3553, DOI: 10.1039/D3SC00102D.
3 P. Chen, C. Chen and T. Yeh, Organic Multiviologen Electrochromic Cells for a Color Electronic Display Application, *J. Appl. Polym. Sci.*, 2014, **131**(13), app.40485, DOI: 10.1002/app.40485.
4 P. M. S. Monk, C. Turner and S. P. Akhtar, Electrochemical Behaviour of Methyl Viologen in a Matrix of Paper, *Electrochim. Acta*, 1999, **44**(26), 4817–4826, DOI: 10.1016/S0013-4686(99)00225-X.
5 K. Madasamy, D. Velayutham, V. Suryanarayanan, M. Kathiresan and K.-C. Ho, Viologen-Based Electrochromic Materials and Devices, *J. Mater. Chem. C*, 2019, **7**(16), 4622–4637, DOI: 10.1039/C9TC00416E.
6 H.-J. Kim, W. S. Jeon, Y. H. Ko and K. Kim, Inclusion of Methylviologen in Cucurbit[7]Uril, *Proc. Natl. Acad. Sci. U. S. A.*, 2002, **99**(8), 5007–5011, DOI: 10.1073/pnas.062656699.
7 C. L. Bird and A. T. Kuhn, Electrochemistry of the Viologens, *Chem. Soc. Rev.*, 1981, **10**(1), 49, DOI: 10.1039/cs9811000049.
8 C. Lee, C. Kim and J. W. Park, Effect of α- and β-Cyclodextrin on the Electrochemistry of Methylheptylviologen and Dibenzylviologen, *J. Electroanal. Chem.*, 1994, **374**(1–2), 115–121, DOI: 10.1016/0022-0728(94)03362-5.
9 R. J. Prankerd, H. W. Stone, K. B. Sloan and J. H. Perrin, Degradation of Aspartame in Acidic Aqueous Media and Its Stabilization by Complexation with Cyclodextrins or Modified Cyclodextrins, *Int. J. Pharm.*, 1992, **88**(1–3), 189–199, DOI: 10.1016/0378-5173(92)90316-T.
10 A. Banga and R. Mitra, Minimization of Shaking-Induced Formation of Insoluble Aggregates of Insulin by Cyclodextrins, *J. Drug Targeting*, 1993, **1**(4), 341–345, DOI: 10.3109/10611869308996093.
11 A. Yasuda, H. Mori and J. Seto, Electrochromic Properties of Alkylviologen-Cyclodextrin Systems, *J. Appl. Electrochem.*, 1987, **17**(3), 567–573, DOI: 10.1007/BF01084131.
12 K. M. Cheah, J. V. Jun, K. D. Wittrup and R. T. Raines, Host–Guest Complexation by β-Cyclodextrin Enhances the Solubility of an Esterified Protein, *Mol. Pharmaceutics*, 2022, **19**(11), 3869–3876, DOI: 10.1021/acs.molpharmaceut.2c00368.
13 J. Lagona, P. Mukhopadhyay, S. Chakrabarti and L. Isaacs, The Cucurbit[*n*]Uril Family, *Angew. Chem., Int. Ed.*, 2005, **44**(31), 4844–4870, DOI: 10.1002/anie.200460675.
14 W. Ong, M. Gómez-Kaifer and A. E. Kaifer, Cucurbit[7]Uril: A Very Effective Host for Viologens and Their Cation Radicals, *Org. Lett.*, 2002, **4**(10), 1791–1794, DOI: 10.1021/ol025869w.
15 P. Dalvand, K. Nchimi Nono, D. Shetty, F. Benyettou, Z. Asfari, C. Platas-Iglesias, M. A. Olson, A. Trabolsi and M. Elhabiri, Viologen–Cucurbituril Host/Guest Chemistry – Redox Control of Dimerization versus Inclusion, *RSC Adv.*, 2021, **11**(47), 29543–29554, DOI: 10.1039/D1RA05488K.
16 B. Ambrose, G. Sathyaraj and M. Kathiresan, Evaluation of the Complexation Behaviour among Functionalized Diphenyl Viologens and Cucurbit[7] and [8]Urils, *Sci. Rep.*, 2024, **14**(1), 5786, DOI: 10.1038/s41598-024-56370-1.
17 S. J. Barrow, S. Kasera, M. J. Rowland, J. Del Barrio and O. A. Scherman, Cucurbituril-Based Molecular Recognition,

Chem. Rev., 2015, **115**(22), 12320–12406, DOI: **10.1021/acs.chemrev.5b00341**.

18 A. E. Kaifer, Toward Reversible Control of Cucurbit[*n*]Uril Complexes, *Acc. Chem. Res.*, 2014, **47**(7), 2160–2167, DOI: **10.1021/ar5001204**.

19 C. Márquez, R. R. Hudgins and W. M. Nau, Mechanism of Host–Guest Complexation by Cucurbituril, *J. Am. Chem. Soc.*, 2004, **126**(18), 5806–5816, DOI: **10.1021/ja0319846**.

20 M. I. El-Barghouthi, K. I. Assaf and A. M. M. Rawashdeh, Molecular Dynamics of Methyl Viologen-Cucurbit[*n*]Uril Complexes in Aqueous Solution, *J. Chem. Theory Comput.*, 2010, **6**(4), 984–992, DOI: **10.1021/ct900622h**.

21 S. R. Peerannawar, V. V. Gobre and S. P. Gejji, Binding of Viologen Derivatives to Cucurbit[8]Uril, *Comput. Theor. Chem.*, 2012, **983**, 16–24, DOI: **10.1016/j.comptc.2011.12.013**.

22 K. Moon and A. E. Kaifer, Modes of Binding Interaction between Viologen Guests and the Cucurbit[7]Uril Host, *Org. Lett.*, 2004, **6**(2), 185–188, DOI: **10.1021/ol035967x**.

23 X. Xiao, Z. Tao, S.-F. Xue, Q.-J. Zhu, J.-X. Zhang, G. A. Lawrance, B. Raguse and G. Wei, Interaction between Cucurbit[8]Uril and Viologen Derivatives, *J. Inclusion Phenom. Macrocyclic Chem.*, 2008, **61**(1–2), 131–138, DOI: **10.1007/s10847-007-9405-1**.

24 W. M. Nau, M. Florea and K. I. Assaf, Deep Inside Cucurbiturils: Physical Properties and Volumes of Their Inner Cavity Determine the Hydrophobic Driving Force for Host–Guest Complexation, *Isr. J. Chem.*, 2011, **51**(5–6), 559–577, DOI: **10.1002/ijch.201100044**.

25 F. Biedermann and O. A. Scherman, Cucurbit[8]Uril Mediated Donor–Acceptor Ternary Complexes: A Model System for Studying Charge-Transfer Interactions, *J. Phys. Chem. B*, 2012, **116**(9), 2842–2849, DOI: **10.1021/jp2110067**.

26 G. Zhu, A. You, H. Song and Z. Li, A Combined Crystallography and DFT Study on Ring-Shaped Cucurbit[*n*]Urils: Structures, Surface Character, and Host–Guest Recognition, *RSC Adv.*, 2022, **12**(16), 10014–10019, DOI: **10.1039/D2RA00797E**.

27 W. S. Jeon, K. Moon, S. H. Park, H. Chun, Y. H. Ko, J. Y. Lee, E. S. Lee, S. Samal, N. Selvapalam, M. V. Rekharsky, V. Sindelar, D. Sobransingh, Y. Inoue, A. E. Kaifer and K. Kim, Complexation of Ferrocene Derivatives by the Cucurbit[7]Uril Host: A Comparative Study of the Cucurbituril and Cyclodextrin Host Families, *J. Am. Chem. Soc.*, 2005, **127**(37), 12984–12989, DOI: **10.1021/ja052912c**.

28 J. W. Lee, S. Samal, N. Selvapalam, H.-J. Kim and K. Kim, Cucurbituril Homologues and Derivatives: New Opportunities in Supramolecular Chemistry, *Acc. Chem. Res.*, 2003, **36**(8), 621–630, DOI: **10.1021/ar020254k**.

29 N. Barooah, J. Mohanty and A. C. Bhasikuttan, Cucurbituril-Based Supramolecular Assemblies: Prospective on Drug Delivery, Sensing, Separation, and Catalytic Applications, *Langmuir*, 2022, **38**(20), 6249–6264, DOI: **10.1021/acs.langmuir.2c00556**.

30 Q. Wu, Q. Lei, H.-C. Zhong, T.-B. Ren, Y. Sun, X.-B. Zhang and L. Yuan, Fluorophore-Based Host–Guest Assembly Complexes for Imaging and Therapy, *Chem. Commun.*, 2023, **59**(21), 3024–3039, DOI: **10.1039/D2CC06286K**.

31 S. J. C. Lee, J. W. Lee, H. H. Lee, J. Seo, D. H. Noh, Y. H. Ko, K. Kim and H. I. Kim, Host–Guest Chemistry from Solution to the Gas Phase: An Essential Role of Direct Interaction with Water for High-Affinity Binding of Cucurbit[*n*]Urils, *J. Phys. Chem. B*, 2013, **117**(29), 8855–8864, DOI: **10.1021/jp4053874**.

32 I. Ghosh and W. M. Nau, The Strategic Use of Supramolecular pKa Shifts to Enhance the Bioavailability of Drugs, *Adv. Drug Delivery Rev.*, 2012, **64**(9), 764–783, DOI: **10.1016/j.addr.2012.01.015**.

33 Y. Zheng and A. E. Kaifer, Kinetics and Thermodynamics of Binding between Zwitterionic Viologen Guests and the Cucurbit[7]Uril Host, *J. Org. Chem.*, 2020, **85**(15), 10240–10244, DOI: **10.1021/acs.joc.0c01201**.

34 F. Biedermann and O. A. Scherman, Cucurbit[8]Uril Mediated Donor–Acceptor Ternary Complexes: A Model System for Studying Charge-Transfer Interactions, *J. Phys. Chem. B*, 2012, **116**(9), 2842–2849, DOI: **10.1021/jp2110067**.

35 I. Osaka, M. Kondou, N. Selvapalam, S. Samal, K. Kim, M. V. Rekharsky, Y. Inoue and R. Arakawa, Characterization of Host–Guest Complexes of Cucurbit[*n*]Uril (*n* = 6, 7) by Electrospray Ionization Mass Spectrometry, *J. Mass Spectrom.*, 2006, **41**(2), 202–207, DOI: **10.1002/jms.978**.

36 P. Bayat, D. Gatineau, D. Lesage, V. Robert, A. Martinez and R. B. Cole, Investigation of Hemicryptophane host–guest Binding Energies Using High-Pressure Collision-Induced Dissociation in Combination with RRKM Modeling, *J. Am. Soc. Mass Spectrom.*, 2019, **30**(3), 509–518, DOI: **10.1007/s13361-018-2109-5**.

37 A. K. Vrkic, R. A. J. O'Hair and C. B. Lebrilla, Unusual Covalent Bond-Breaking Reactions of β-Cyclodextrin Inclusion Complexes of Nucleobases/Nucleosides and Related Guest Molecules, *Eur. J. Mass Spectrom.*, 2003, **9**(6), 563–577, DOI: **10.1255/ejms.589**.

38 G. Carroy, V. Lemaur, J. De Winter, L. Isaacs, E. De Pauw, J. Cornil and P. Gerbaux, Energy-Resolved Collision-Induced Dissociation of Non-Covalent Ions: Charge- and Guest-Dependence of Decomplexation Reaction Efficiencies, *Phys. Chem. Chem. Phys.*, 2016, **18**(18), 12557–12568, DOI: **10.1039/C6CP01026A**.

39 A. K. Vrkic and R. A. J. O'Hair, Using Non-Covalent Complexes to Direct the Fragmentation of Glycosidic Bonds in the Gas Phase, *J. Am. Soc. Mass Spectrom.*, 2004, **15**(5), 715–724, DOI: **10.1016/j.jasms.2004.01.008**.

40 C. A. Schalley, Supramolecular Chemistry Goes Gas Phase: The Mass Spectrometric Examination of Noncovalent Interactions in Host–Guest Chemistry and Molecular Recognition, *Int. J. Mass Spectrom.*, 2000, **194**(1), 11–39, DOI: **10.1016/S1387-3806(99)00243-2**.

41 U. Rauwald, F. Biedermann, S. Deroo, C. V. Robinson and O. A. Scherman, Correlating Solution Binding and ESI-MS Stabilities by Incorporating Solvation Effects in a Confined Cucurbit[8]Uril System, *J. Phys. Chem. B*, 2010, **114**(26), 8606–8615, DOI: **10.1021/jp102933h**.

42 Y. Dotsikas and Y. L. Loukas, Efficient Determination and Evaluation of Model Cyclodextrin Complex Binding Constants by Electrospray Mass Spectrometry, *J. Am. Soc. Mass Spectrom.*, 2003, **14**(10), 1123–1129, DOI: **10.1016/S1044-0305(03)00451-3**.

43 S. Bhattacharya, A. Barba-Bon, T. A. Zewdie, A. B. Müller, T. Nisar, A. Chmielnicka, I. A. Rutkowska, C. J. Schürmann, V. Wagner, N. Kuhnert, P. J. Kulesza, W. M. Nau and U. Kortz, Discrete, Cationic Palladium(II)-Oxo Clusters *via* f-Metal Ion Incorporation and Their Macrocyclic Host–Guest Interactions with Sulfonatocalixarenes, *Angew. Chem., Int. Ed.*, 2022, **61**(25), e202203114, DOI: **10.1002/anie.202203114**.

44 J. L. Casas-Hinestroza, M. Bueno, E. Ibáñez and A. Cifuentes, Recent Advances in Mass Spectrometry Studies of Non-Covalent Complexes of Macrocycles – A Review, *Anal. Chim. Acta*, 2019, **1081**, 32–50, DOI: **10.1016/j.aca.2019.06.029**.

45 P. Su, A. J. Smith, J. Warneke and J. Laskin, Gas-Phase Fragmentation of host–guest Complexes of Cyclodextrins and Polyoxometalates, *J. Am. Soc. Mass Spectrom.*, 2019, **30**(10), 1934–1945, DOI: **10.1007/s13361-019-02266-8**.

46 P. Su, X. Zhu, S. M. Wilson, Y. Feng, H. Y. Samayoa-Oviedo, C. Sonnendecker, A. J. Smith, W. Zimmermann and J. Laskin, The Effect of Host Size on Binding in Host–Guest Complexes of Cyclodextrins and Polyoxometalates, *Chem. Sci.*, 2024, **15**(30), 11825–11836, DOI: **10.1039/D4SC01061B**.

47 T.-C. Lee, E. Kalenius, A. I. Lazar, K. I. Assaf, N. Kuhnert, C. H. Grün, J. Jänis, O. A. Scherman and W. M. Nau, Chemistry inside Molecular Containers in the Gas Phase, *Nat. Chem.*, 2013, **5**(5), 376–382, DOI: **10.1038/nchem.1618**.

48 D. L. Marshall, B. L. J. Poad, E. T. Luis, R. A. Da Silva Rodrigues, S. J. Blanksby and K. M. Mullen, Stepwise Reduction of Interlocked Viologen-Based Complexes in the Gas Phase, *Chem. Commun.*, 2020, **56**(88), 13575–13578, DOI: **10.1039/D0CC05115B**.

49 L. Cera and C. A. Schalley, Supramolecular Reactivity in the Gas Phase: Investigating the Intrinsic Properties of Non-Covalent Complexes, *Chem. Soc. Rev.*, 2014, **43**(6), 1800, DOI: **10.1039/c3cs60360a**.

50 H. D. F. Winkler, E. V. Dzyuba, A. Springer, L. Losensky and C. A. Schalley, Gas-Phase Organocatalysis with Crown Ethers, *Chem. Sci.*, 2012, **3**(4), 1111, DOI: **10.1039/c2sc00796g**.

51 J. Shrestha, S. R. Porter, C. Tinsley, A. J. Arslanian and D. V. Dearden, Prototypical Allosterism in a Simple Ditopic Ligand: Gas-Phase Topologies of Cucurbit[n]Uril· n -Alkylammonium Complexes Controlled by Binding in the Second Site, *J. Phys. Chem. A*, 2022, **126**(19), 2950–2958, DOI: **10.1021/acs.jpca.2c01703**.

52 A. Saura-Sanmartin and C. A. Schalley, The Mobility of Homomeric Lasso- and Daisy Chain-Like Rotaxanes in Solution and in the Gas Phase as a Means to Study Structure and Switching Behaviour, *Isr. J. Chem.*, 2023, **63**(7–8), e202300022, DOI: **10.1002/ijch.202300022**.

53 B. Brusilowskij, S. Neubacher and C. A. Schalley, A Double Intramolecular Cage Contraction within a Self-Assembled Metallo-Supramolecular Bowl, *Chem. Commun.*, 2009, 785, DOI: **10.1039/b819412b**.

54 L. Polewski, A. Springer, K. Pagel and C. A. Schalley, Gas-Phase Structural Analysis of Supramolecular Assemblies, *Acc. Chem. Res.*, 2021, **54**(10), 2445–2456, DOI: **10.1021/acs.accounts.1c00080**.

55 L. Jiang, R. T. Hilger and J. Laskin, Hardware and Software Solutions for Implementing Nanospray Desorption Electrospray Ionization (nano-DESI) Sources on Commercial Mass Spectrometers, *J. Mass Spectrom.*, 2024, **59**(7), e5065, DOI: **10.1002/jms.5065**.

56 L. Patiny and A. Borel, ChemCalc: A Building Block for Tomorrow's Chemical Infrastructure, *J. Chem. Inf. Model.*, 2013, **53**(5), 1223–1228, DOI: **10.1021/ci300563h**.

57 C. Lifshitz, Kinetic Shifts, *Eur. J. Mass Spectrom.*, 2002, **8**(2), 85–98, DOI: **10.1255/ejms.476**.

58 J. Laskin, Energy and Entropy Effects in Gas-Phase Dissociation of Peptides and Proteins, in *Principles of Mass Spectrometry Applied to Biomolecules*, ed. J. Laskin and C. Lifshitz, Wiley, 2006, pp. 619–665, DOI: **10.1002/047005042X.ch16**.

59 M. J. Frisch, G. W. Trucks, H. B. Schlegel, G. E. Scuseria, M. A. Robb, J. R. Cheeseman, G. Scalmani, V. Barone, G. A. Petersson, H. Nakatsuji, X. Li, M. Caricato, A. V. Marenich, J. Bloino, B. G. Janesko, R. Gomperts, B. Mennucci, H. P. Hratchian, J. V. Ortiz, A. F. Izmaylov, J. L. Sonnenberg, D. Williams-Young, F. Ding, F. Lipparini, F. Egidi, J. Goings, B. Peng, A. Petrone, T. Henderson, D. Ranasinghe, V. G. Zakrzewski, J. Gao, N. Rega, G. Zheng, W. Liang, M. Hada, M. Ehara, K. Toyota, R. Fukuda, J. Hasegawa, M. Ishida, T. Nakajima, Y. Honda, O. Kitao, H. Nakai, T. Vreven, K. Throssell, J. A. Montgomery Jr., J. E. Peralta, F. Ogliaro, M. J. Bearpark, J. J. Heyd, E. N. Brothers, K. N. Kudin, V. N. Staroverov, T. A. Keith, R. Kobayashi, J. Normand, K. Raghavachari, A. P. Rendell, J. C. Burant, S. S. Iyengar, J. Tomasi, M. Cossi, J. M. Millam, M. Klene, C. Adamo, R. Cammi, J. W. Ochterski, R. L. Martin, K. Morokuma, O. Farkas, J. B. Foresman and D. J. Fox, *Gaussian 16 Rev. C.01*, 2016.

60 Z. B. Maksić, B. Kovačević and R. Vianello, Advances in Determining the Absolute Proton Affinities of Neutral Organic Molecules in the Gas Phase and Their Interpretation: A Theoretical Account, *Chem. Rev.*, 2012, **112**(10), 5240–5270, DOI: **10.1021/cr100458v**.

61 D. Zhang, J. Tian, L. Chen, L. Zhang and Z. Li, Dimerization of Conjugated Radical Cations: An Emerging Non-Covalent Interaction for Self-Assembly, *Chem. – Asian J.*, 2015, **10**(1), 56–68, DOI: **10.1002/asia.201402805**.

62 C. Gong, D. Li, X. Li, D. Zhang, D. Xing, L. Zhao, X. Yuan and X. Zhang, Spontaneous Reduction-Induced Degradation of Viologen Compounds in Water Microdroplets and Its Inhibition by Host–Guest Complexation, *J. Am. Chem. Soc.*, 2022, **144**(8), 3510–3516, DOI: **10.1021/jacs.1c12028**.

63 K. Levsen, Isomerisation of Hydrocarbon Ions:I—Isomeric Octanes: Acollisional Actiation Study, *Org. Mass Spectrom.*, 1975, **10**(1), 43–54, DOI: **10.1002/oms.1210100108**.

64 A. Lavanchy, R. Houriet and T. Gäumann, The Mass Spectrometric Fragmentation of *n*-heptane, *Org. Mass Spectrom.*, 1978, **13**(7), 410–416, DOI: **10.1002/oms.1210130709**.

65 D. Stahl and T. Gäuumann, The Mass Spectrum of 1-heptyl Iodide, *Org. Mass Spectrom.*, 1977, **12**(12), 761–765, DOI: **10.1002/oms.1210121211**.

66 C. H. DePuy, S. Gronert, S. E. Barlow, V. M. Bierbaum and R. Damrauer, The Gas-Phase Acidities of the Alkanes, *J. Am. Chem. Soc.*, 1989, **111**(6), 1968–1973, DOI: **10.1021/ja00188a003**.

67 S. Sieber, P. Buzek, P. V. R. Schleyer, W. Koch and J. W. D. M. Carneiro, The *Tert*-Butyl Cation ($C_4H_9^+$) Potential Energy Surface, *J. Am. Chem. Soc.*, 1993, **115**(1), 259–270, DOI: **10.1021/ja00054a037**.

68 A. Lavanchy, R. Houriet and T. Gäumann, The Mass Spectrometric Fragmentation of *n*-alkanes, *Org. Mass Spectrom.*, 1979, **14**(2), 79–85, DOI: **10.1002/oms.1210140205**.

69 D. H. Noh, S. J. C. Lee, J. W. Lee and H. I. Kim, Host–Guest Chemistry in the Gas Phase: Complex Formation of Cucurbit[6]Uril with Proton-Bound Water Dimer, *J. Am. Soc. Mass Spectrom.*, 2014, **25**(3), 410–421, DOI: **10.1007/s13361-013-0795-6**.

70 D. K. S. Sharma and P. Kebarle, Stability and Reactivity of the Benzyl and Tropylium Cations in the Gas Phase, *Can. J. Chem.*, 1981, **59**(11), 1592–1601, DOI: **10.1139/v81-235**.

71 J. L. M. Abbound, W. J. Hehre and R. W. Taft, Benzyl Cation. A Long-Lived Species in the Gas Phase?, *J. Am. Chem. Soc.*, 1976, **98**(19), 6072–6073, DOI: **10.1021/ja00435a067**.

72 D. Schröder and H. Schwarz, Generation, Stability, and Reactivity of Small, Multiply Charged Ions in the Gas Phase, *J. Phys. Chem. A*, 1999, **103**(37), 7385–7394, DOI: **10.1021/jp991332x**.

73 G. McCartney, T. Hacker and B. Yang, Empowering Faculty: A Campus Cyberinfrastructure Strategy for Research Communities, *Educ. Rev.*, 2014, **https://er.educause.edu/articles/2014/7/empowering-faculty-a-campus-cyberinfrastructure-strategy-for-research-communities**.